Supplemental Information for:

Forced Self-Modification Assays as a Strategy to Screen MonoPARP Enzymes

Tim J. Wigle*[1], W. David Church[1], Christina R. Majer[1], Kerren K. Swinger[1], Demet Aybar[1], Laurie B. Schenkel[1], Melissa M. Vasbinder[1], Arne Brendes[2], Claudia Beck[2], Martin Prahm[2], Dennis Wegener[2], Paul Chang[1] and Kevin W. Kuntz[1]

[1]Ribon Therapeutics Inc., 35 Cambridgepark Drive, Cambridge, Massachusetts, USA, 02140

[2]Evotec AG, Manfred Eigen Campus, Essener Bogen 7, Hamburg, Germany, 22419

*To whom correspondence should be addressed

twigle@ribontx.com

Supplemental Figure S1 – PARP Phylogenetic Tree

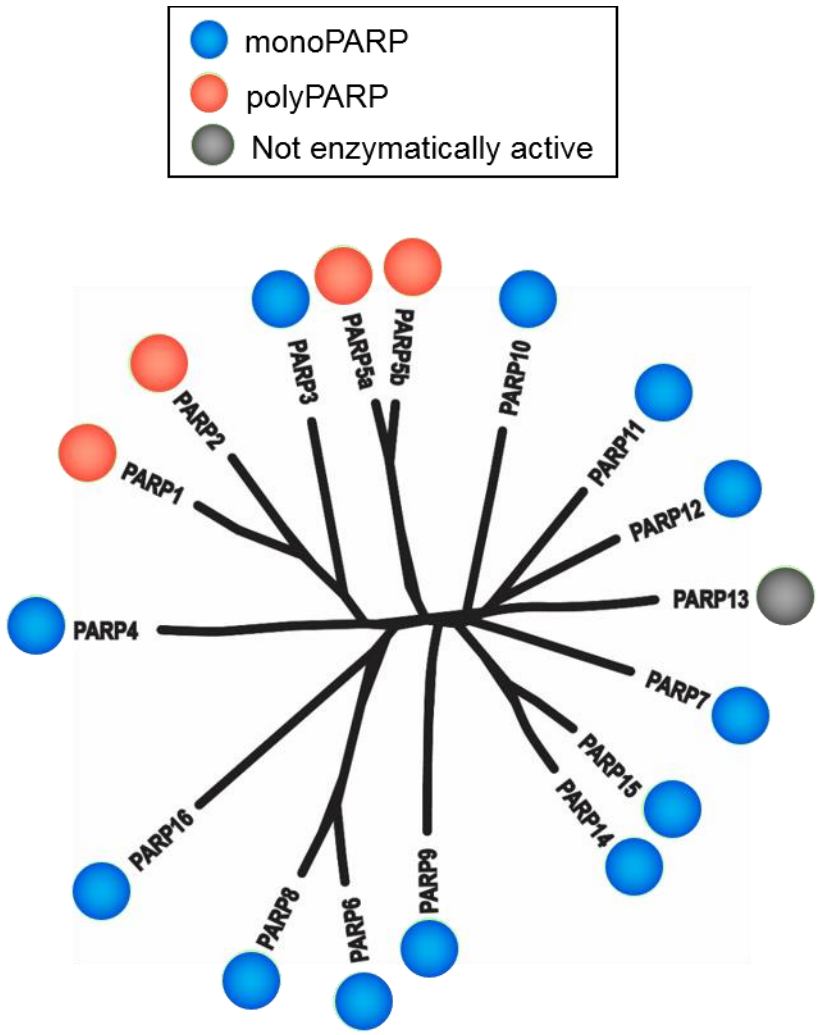

Figure S1. Phylogenetic tree of 17 human PARPs created using the amino acid sequence of the defined catalytic PARP domains. The proteins are sub-classified as monoPARPs, polyPARPs or not enzymatically active.

Supplemental Figure S2 – PARP Publications

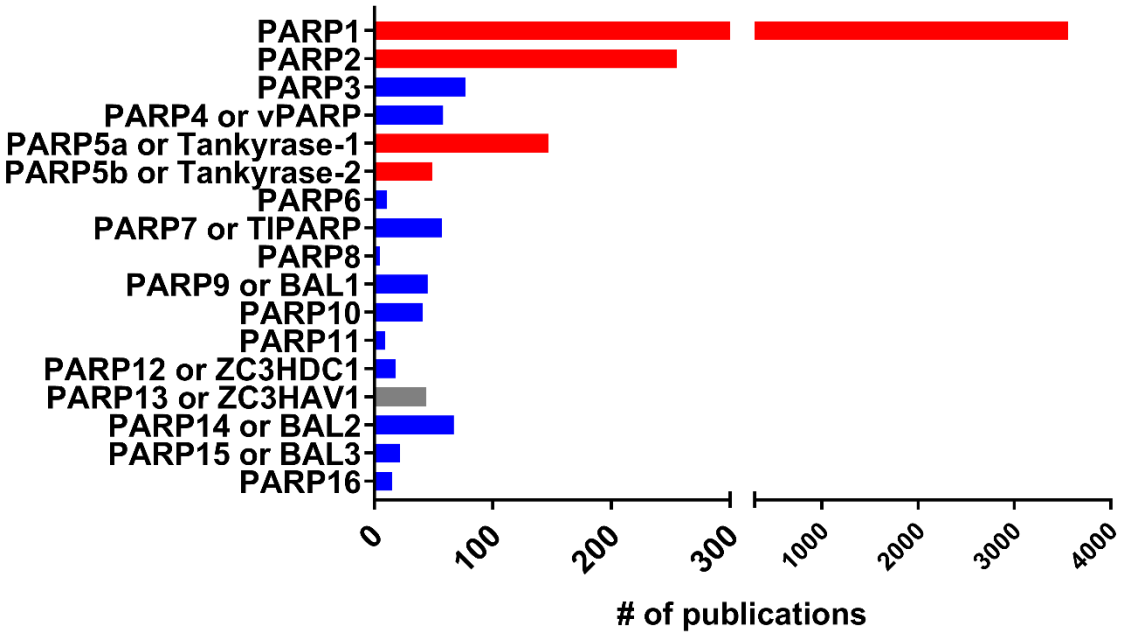

Figure S2. Number of peer-reviewed publications indexed on Pubmed as of August 15, 2019 existing for monoPARPs (blue bars) or polyPARPs (red bars). PARP13 (grey bar) has not been shown to be enzymatically active. The search term entered for each PARP is listed on the y-axis.

Supplemental Figure S3 – Measuring incorporation of ^{32}P-NAD^{+} to reported substrates of PARP1 and PARP16.

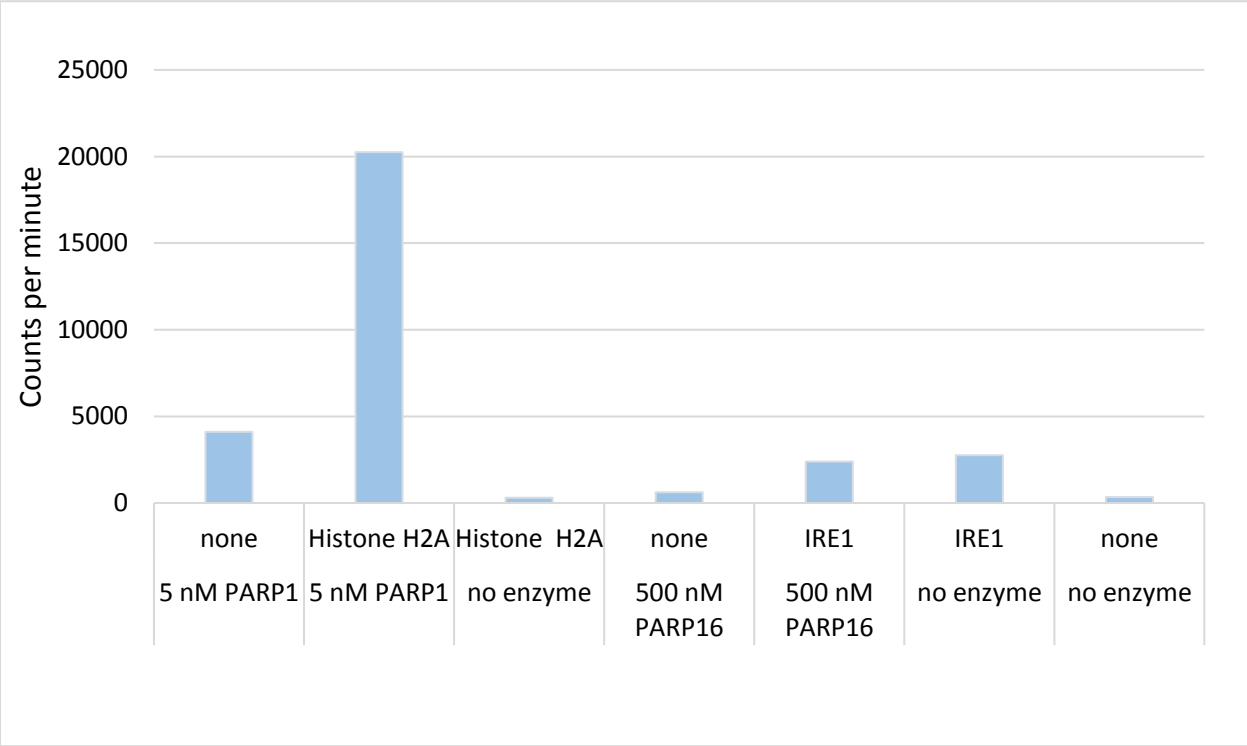

Figure S3. Reactions were run in a 50 µL volume at 25 °C in a buffer of 20 mM HEPES (pH = 7.5), 100 mM NaCl, 2 mM DTT, 0.1% DTPA-purified BSA and 0.002% Tween 20. The indicated amount of each enzyme was mixed with 500 nM of either histone H2A or IRE1 (BPS Biosciences; San Diego, CA), along with 500 nM ^{32}P-NAD^{+} (American Radiolabeled Chemical; St. Louis, MO)**.** Reactions were terminated by precipitating with 600 µL of 20% trichloroacetic acid (TCA), chilling on ice for 5 minutes, then centrifuging to form a pellet. The TCA was removed, and 5 mL of scintillation fluid was added and incorporation of the ^{32}P was measured on a scintillation proximity counter. Signficant increase scintillation counts was only detected in the PARP1 – histone H2A reaction and PARP1 by itself reactions, however the magnitude of signal was greater when histone H2A was present.

Supplemental Figure S4 – PARP1 Assay Development

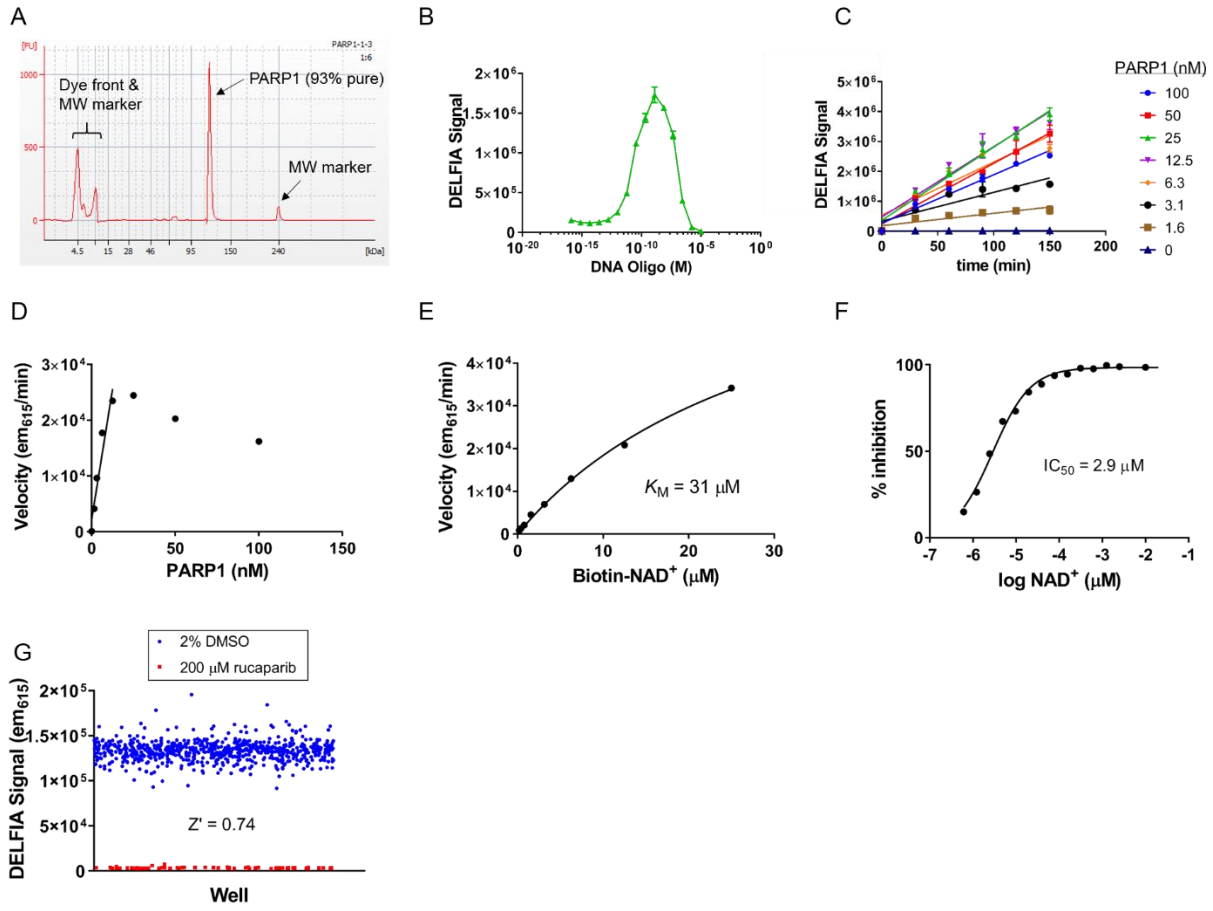

Figure S4. A) Recombinant PARP1 purified from *Sf9* cells via a His6 tag was 93% pure as judged by capillary electrophoresis. B) PARP1 activation seen as a synthetic oligonucleotide is titrated. C) Linearity of product formation vs. time was evaluated at multiple enzyme concentrations. D) Velocity vs. enzyme concentration was plotted and the linear range of this relationship goes up to 12.5 nM enzyme. E) The K_M^{app} for biotin-NAD$^+$ was measured to be 31 µM. F) Unlabeled NAD$^+$ outcompetes incorporation of biotinylated NAD$^+$ under final assay conditions with an IC_{50} of 2.9 µM. G) Uniformity experiments were performed using the final assay conditions and the assay was robust and reproducible as judged by a Z' of 0.74.

Supplemental Figure S5 – PARP2 Assay Development

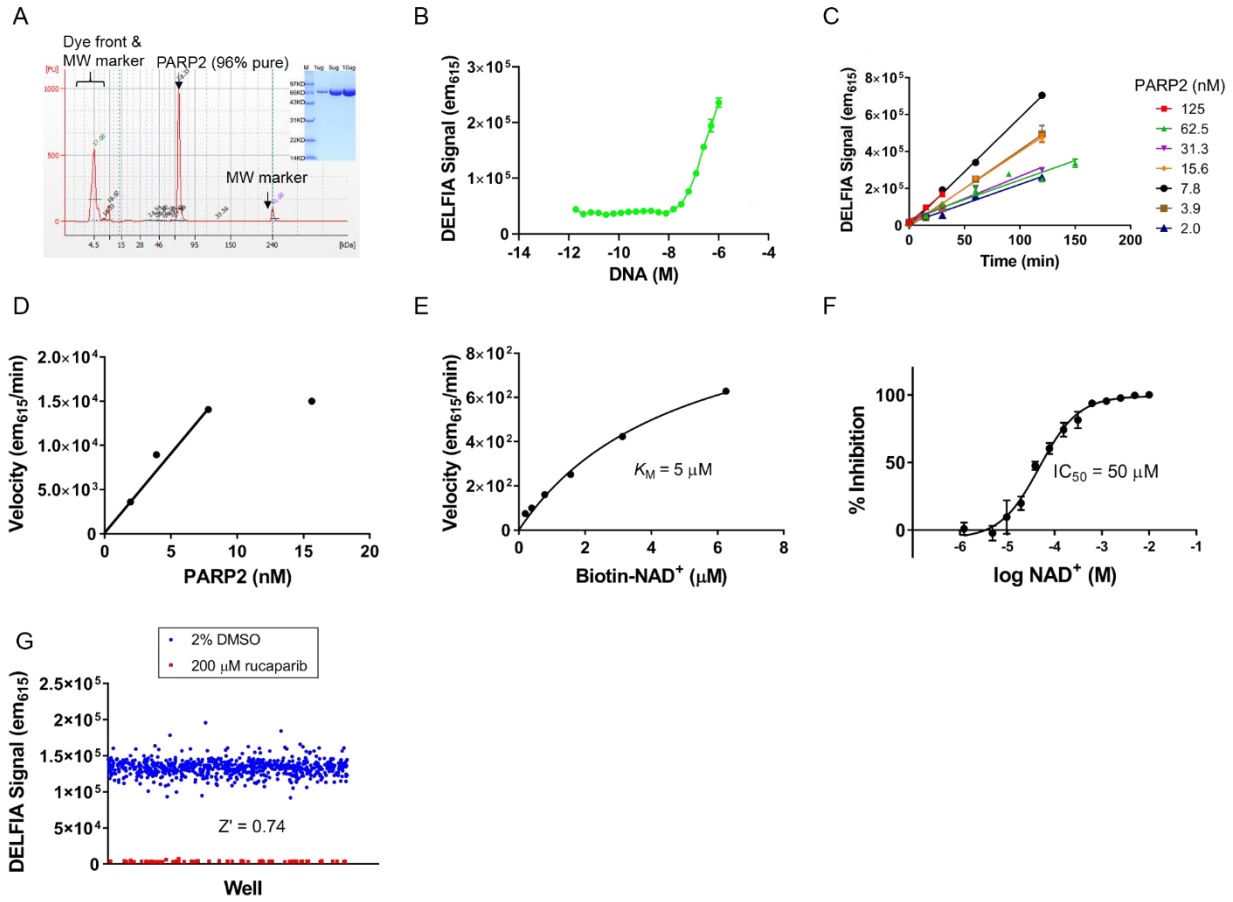

Figure S5. A) Recombinant PARP2 purified from *Sf9* cells via a His6 tag was 96% pure as judged by capillary electrophoresis (main) and SDS-PAGE (inset). B) PARP2 activation seen as a synthetic oligonucleotide is titrated. C) Linearity of product formation vs. time was evaluated at multiple enzyme concentrations. D) Velocity vs. enzyme concentration was plotted and the linear range of this relationship goes up to 7.5 nM enzyme. E) The K_M^{app} for biotin-NAD$^+$ was measured to be 5 µM. F) Unlabeled NAD$^+$ outcompetes incorporation of biotinylated NAD$^+$ under final assay conditions with an IC_{50} of 50 µM. G) Uniformity experiments were performed using the final assay conditions and the assay was robust and reproducible as judged by a Z' of 0.74.

Supplemental Figure S6 – PARP3 Assay Development

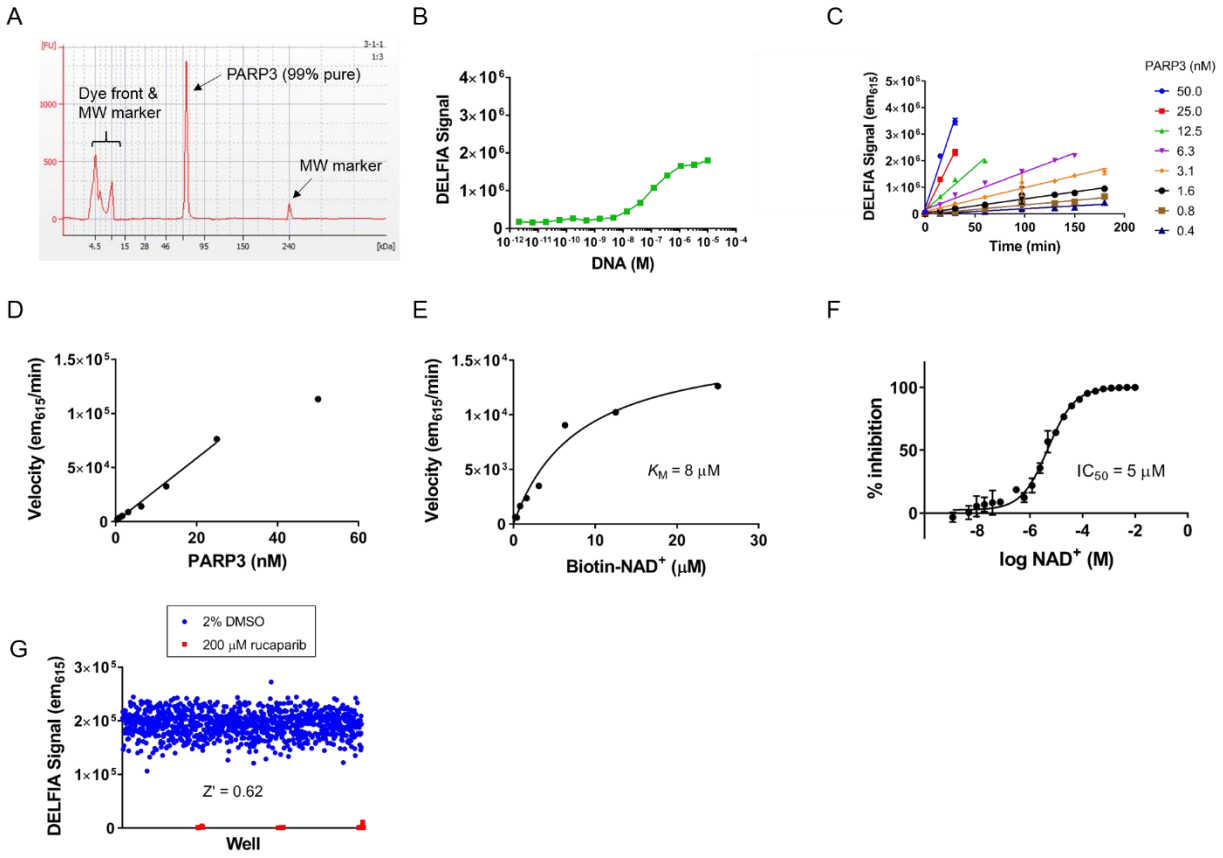

Figure S6. A) Recombinant PARP3 enzyme purified from *E. coli* via a His6 tag was 99% pure as judged by capillary electrophoresis. B) PARP3 activation seen as a synthetic oligonucleotide is titrated. C) Linearity of product formation vs. time was evaluated at multiple enzyme concentrations. D) Velocity vs. enzyme concentration was plotted and the linear range of this relationship goes up to 25 nM enzyme. E) The K_M^{app} for biotin-NAD$^+$ was measured to be 8 µM. F) Unlabeled NAD$^+$ outcompetes incorporation of biotinylated NAD$^+$ under final assay conditions with an IC_{50} of 5 µM. G) Uniformity experiments were performed using the final assay conditions and the assay was robust and reproducible as judged by a Z' of 0.62.

Supplemental Figure S7 – PARP4 Assay Development

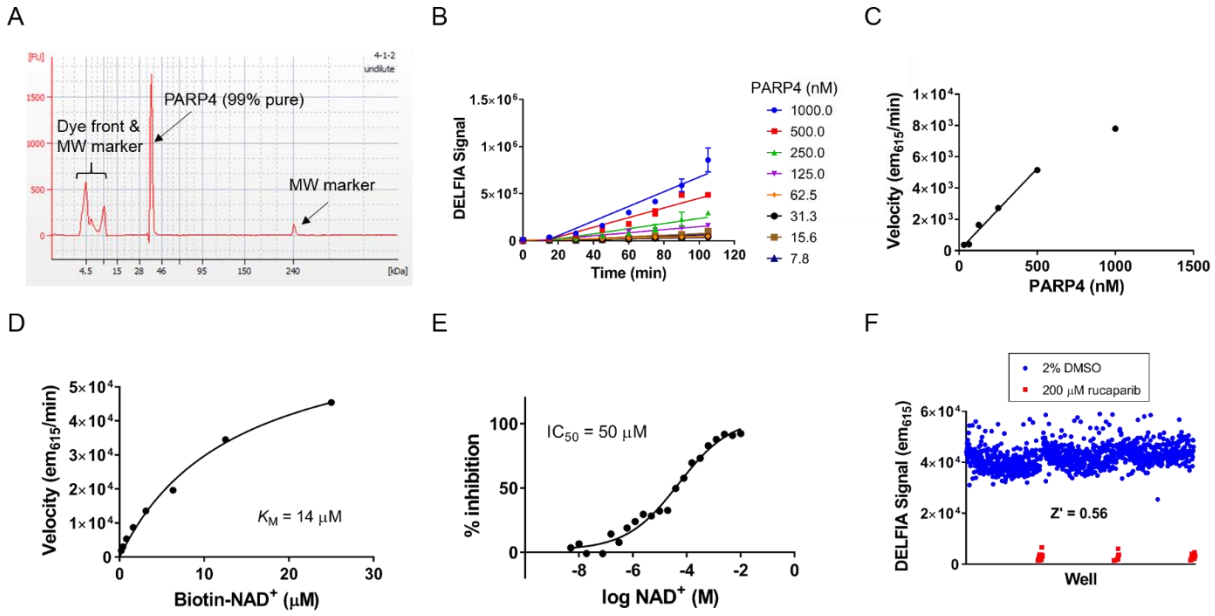

Figure S7. A) Recombinant PARP4 purified from *Sf21* cells via a His6 tag was 99% pure as judged by capillary electrophoresis. B) Linearity of product formation vs. time was evaluated at multiple enzyme concentrations. C) Velocity vs. enzyme concentration was plotted and the linear range of this relationship goes up to 500 nM enzyme. D) The K_M^{app} for biotin-NAD$^+$ was measured to be 14 µM. E) Unlabeled NAD$^+$ outcompetes incorporation of biotinylated NAD$^+$ under final assay conditions with an IC_{50} of 50 µM. F) Uniformity experiments were performed using the final assay conditions and the assay was robust and reproducible as judged by a Z' of 0.56.

Supplemental Figure S8 – PARP5a Assay Development

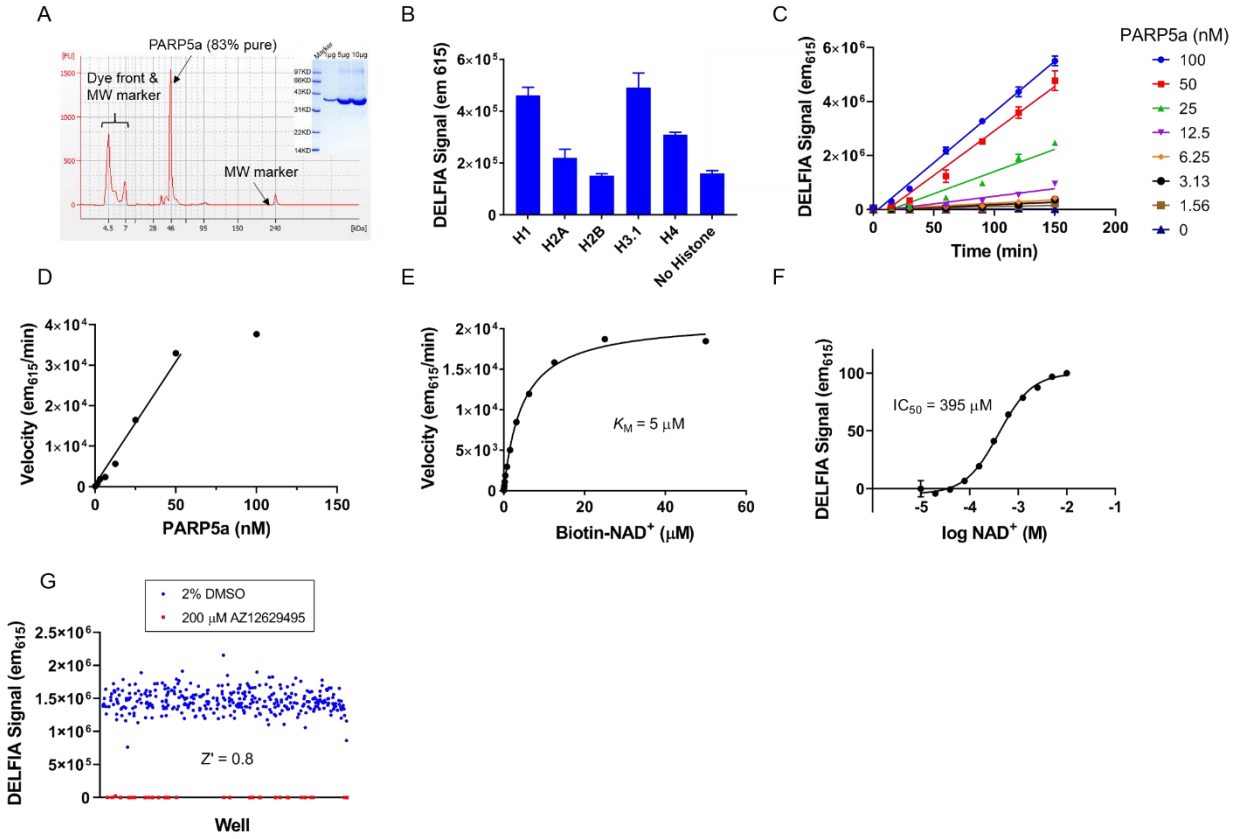

Figure S8. A) Recombinant PARP5a purified from *Sf9* cells via a His6 tag was 83% pure as judged by capillary electrophoresis (main) and SDS-PAGE (inset). B) Histone H1 and H3.1 were the most robust substrates for PARP5a, and histone H1 was selected for further assay development. C) Linearity of product formation vs. time was evaluated at multiple enzyme concentrations. D) Velocity vs. enzyme concentration was plotted and the linear range of this relationship goes up to 50 nM enzyme. E) The K_M^{app} for biotin-NAD$^+$ was measured to be 5 µM. F) Unlabeled NAD$^+$ outcompetes incorporation of biotinylated NAD$^+$ under final assay conditions with an IC_{50} of 395 µM. G) Uniformity experiments were performed using the final assay conditions and the assay was robust and reproducible as judged by a Z' of 0.8.

Supplemental Figure S9 – PARP6 Assay Development

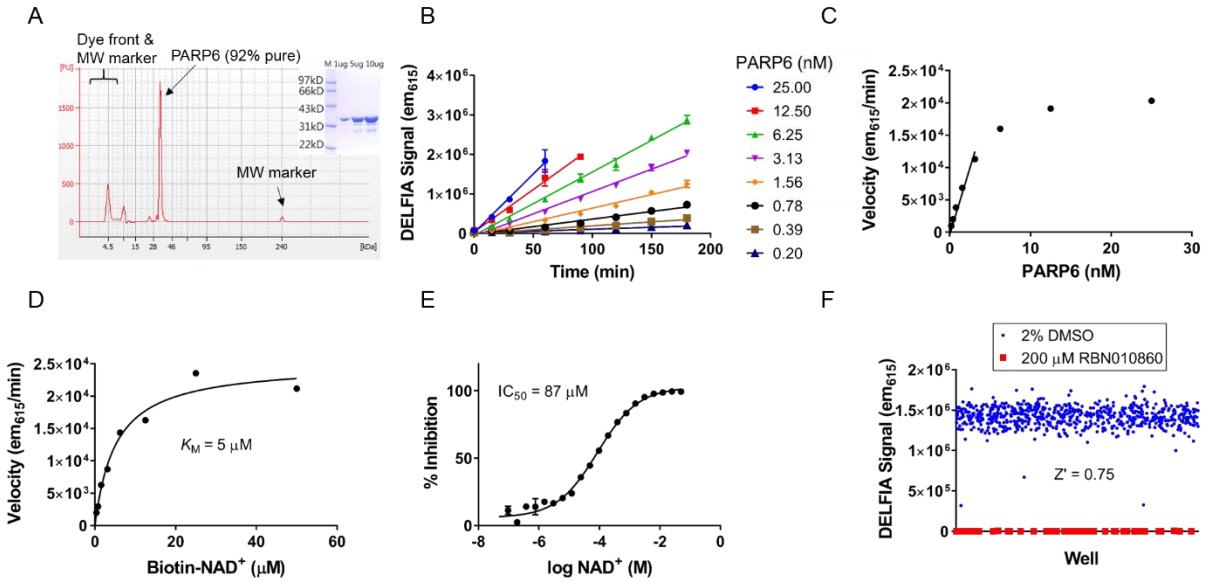

Figure S9. A) Recombinant PARP6 purified from *E. coli* via a His6 tag was 92% pure as judged by capillary electrophoresis (main) and SDS-PAGE (inset). B) Linearity of product formation vs. time was evaluated at multiple enzyme concentrations. C) Velocity vs. enzyme concentration was plotted and the linear range of this relationship goes up to 3 nM enzyme. D) The K_M^{app} for biotin-NAD$^+$ was measured to be 5 µM. E) Unlabeled NAD$^+$ outcompetes incorporation of biotinylated NAD$^+$ under final assay conditions with an IC_{50} of 87 µM. F) Uniformity experiments were performed using the final assay conditions and the assay was robust and reproducible as judged by a Z' of 0.75.

Supplemental Figure S10 – PARP7 Assay Development

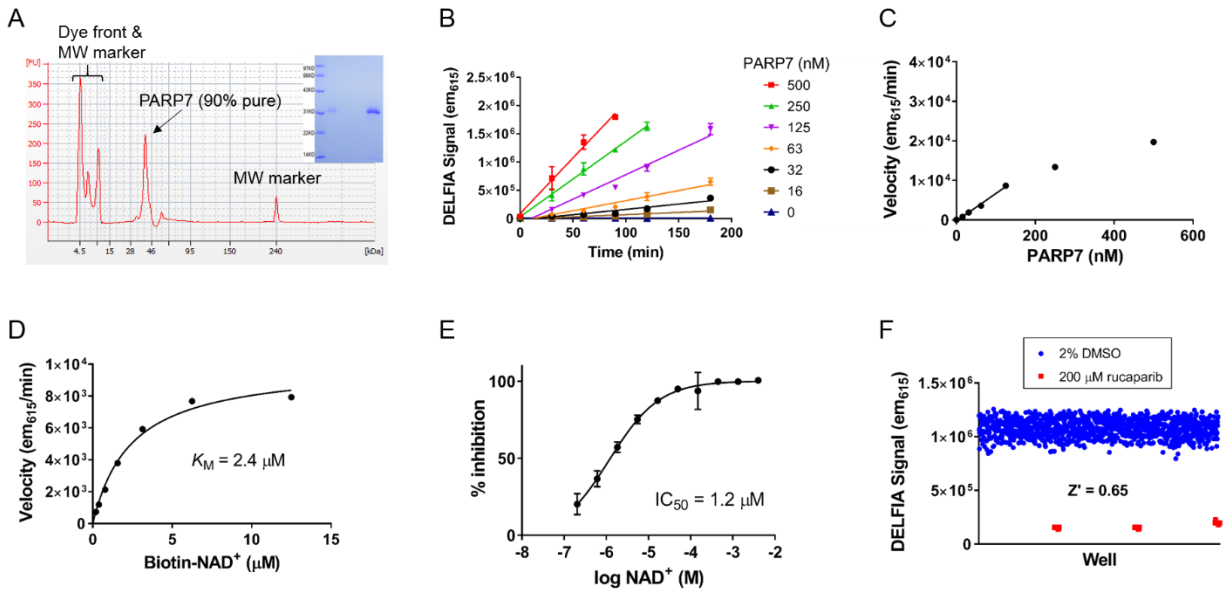

Figure S10. A) Recombinant PARP7 purified from *E. coli* via a His6 tag was 90% pure as judged by capillary electrophoresis (main) and SDS-PAGE (inset). B) Linearity of product formation vs. time was evaluated at multiple enzyme concentrations. C) Velocity vs. enzyme concentration was plotted and the linear range of this relationship goes up to 125 nM enzyme. D) The K_M^{app} for biotin-NAD$^+$ was measured to be 2.4 µM. E) Unlabeled NAD$^+$ outcompetes incorporation of biotinylated NAD$^+$ under final assay conditions with an IC_{50} of 1.2 µM. F) Uniformity experiments were performed using the final assay conditions and the assay was robust and reproducible as judged by a Z' of 0.65.

Supplemental Figure S11 – PARP8 Assay Development

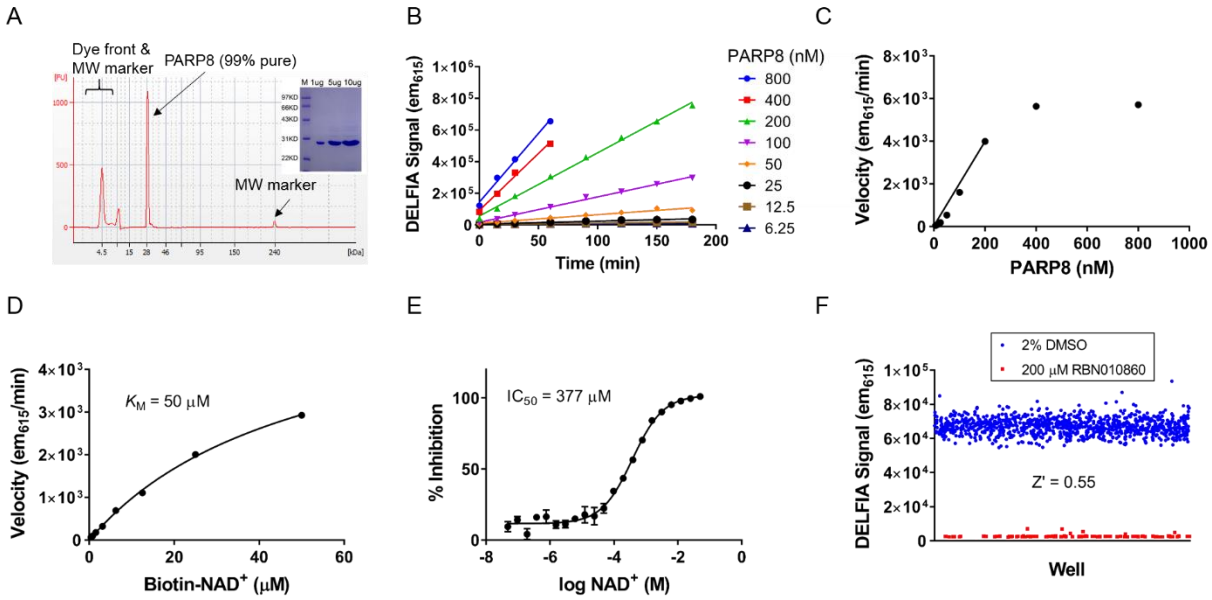

Figure S11. A) Recombinant PARP8 purified from *E. coli* via a His6 tag was 99% pure as judged by capillary electrophoresis (main) and SDS-PAGE (inset). B) Linearity of product formation vs. time was evaluated at multiple enzyme concentrations. C) Velocity vs. enzyme concentration was plotted and the linear range of this relationship goes up to 200 nM enzyme. D) The K_M^{app} for biotin-NAD$^+$ was measured to be 50 µM. E) Unlabeled NAD$^+$ outcompetes incorporation of biotinylated NAD$^+$ under final assay conditions with an IC_{50} of 377 µM. F) Uniformity experiments were performed using the final assay conditions and the assay was robust and reproducible as judged by a Z' of 0.55.

Supplemental Figure S12 – PARP10 Assay Development

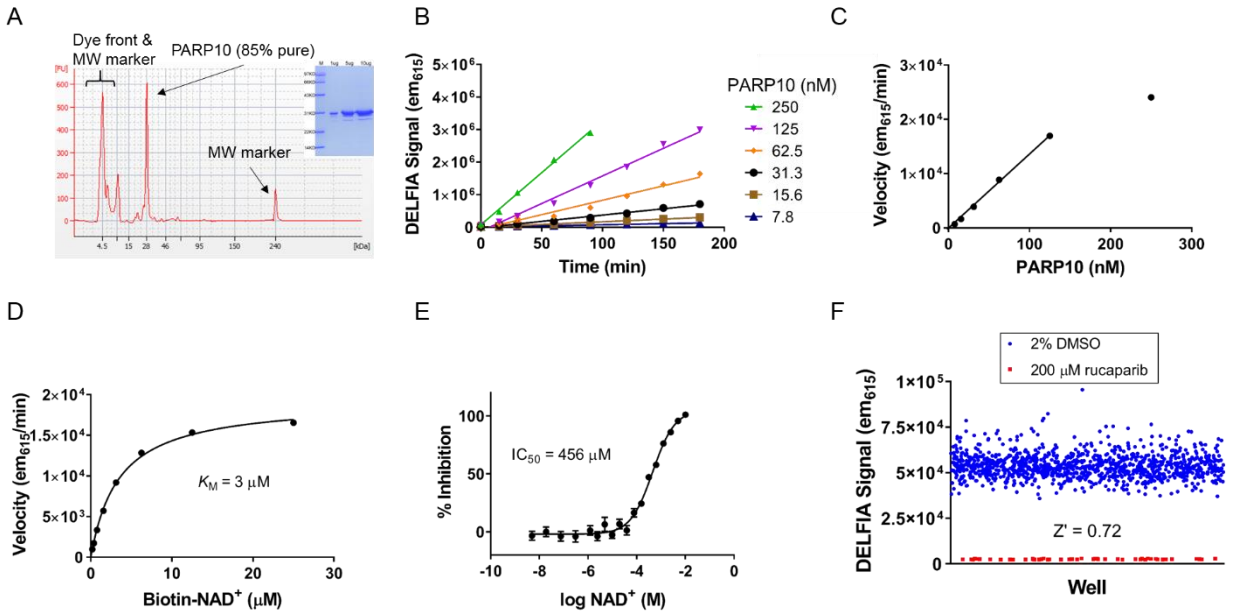

Figure S12. A) Recombinant PARP10 purified from *E. coli* via a His6 tag was 85% pure as judged by capillary electrophoresis (main) and SDS-PAGE (inset). B) Linearity of product formation vs. time was evaluated at multiple enzyme concentrations. C) Velocity vs. enzyme concentration was plotted and the linear range of this relationship goes up to 125 nM enzyme. D) The K_M^{app} for biotin-NAD$^+$ was measured to be 3 µM. E) Unlabeled NAD$^+$ outcompetes incorporation of biotinylated NAD$^+$ under final assay conditions with an IC_{50} of 456 µM. F) Uniformity experiments were performed using the final assay conditions and the assay was robust and reproducible as judged by a Z' of 0.72.

Supplemental Figure S13 – PARP11 Assay Development

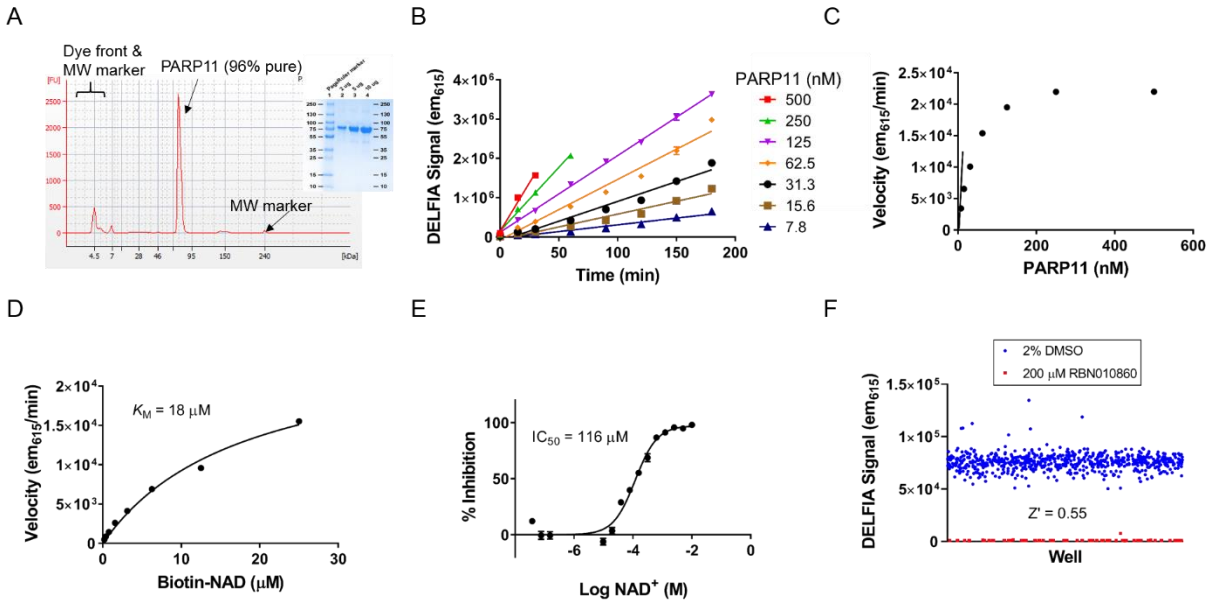

Figure S13. A) Recombinant PARP11 purified from *Sf21* cells via a His6 tag was 96% pure as judged by capillary electrophoresis (main) and SDS-PAGE (inset). B) Linearity of product formation vs. time was evaluated at multiple enzyme concentrations. C) Velocity vs. enzyme concentration was plotted and the linear range of this relationship goes up to 16 nM enzyme. D) The K_M^{app} for biotin-NAD$^+$ was measured to be 18 µM. E) Unlabeled NAD$^+$ outcompetes incorporation of biotinylated NAD$^+$ under final assay conditions with an IC_{50} of 116 µM. F) Uniformity experiments were performed using the final assay conditions and the assay was robust and reproducible as judged by a Z' of 0.55.

Supplemental Figure S14 – PARP12 Assay Development

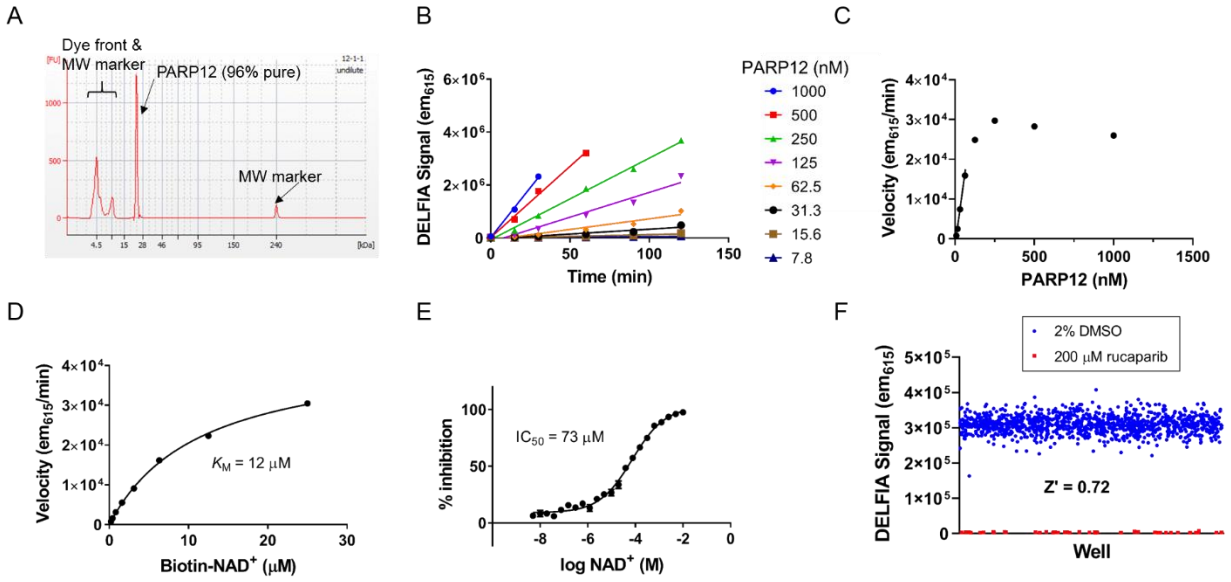

Figure S14. A) Recombinant PARP12 purified from *Sf9* cells via a His6 tag was 96% pure as judged by capillary electrophoresis (main). B) Linearity of product formation vs. time was evaluated at multiple enzyme concentrations. C) Velocity vs. enzyme concentration was plotted and the linear range of this relationship goes up to 62 nM enzyme. D) The K_M^{app} for biotin-NAD$^+$ was measured to be 12 µM. E) Unlabeled NAD$^+$ outcompetes incorporation of biotinylated NAD$^+$ under final assay conditions with an IC_{50} of 73 µM. F) Uniformity experiments were performed using the final assay conditions and the assay was robust and reproducible as judged by a Z' of 0.72.

Supplemental Figure S15 – PARP14 Assay Development

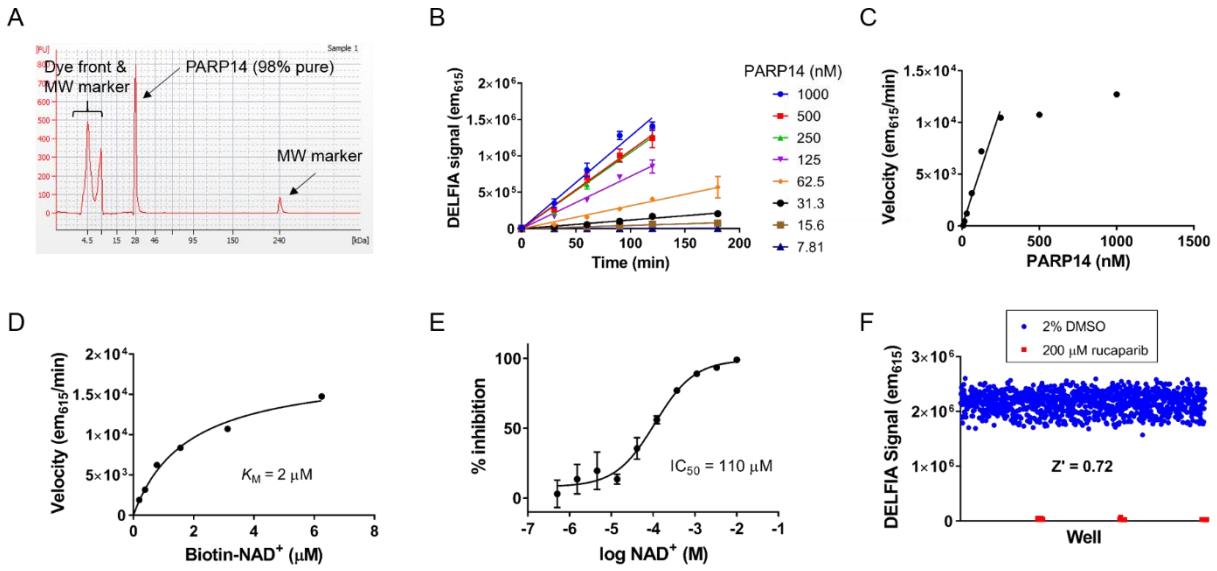

Figure S15. A) Recombinant PARP14 purified from *E. coli* via a His6 tag was 98% pure as judged by capillary electrophoresis. B) Linearity of product formation vs. time was evaluated at multiple enzyme concentrations. C) Velocity vs. enzyme concentration was plotted and the linear range of this relationship goes up to 250 nM enzyme. D) The K_M^{app} for biotin-NAD$^+$ was measured to be 2 µM. E) Unlabeled NAD$^+$ outcompetes incorporation of biotinylated NAD$^+$ under final assay conditions with an IC_{50} of 110 µM. F) Uniformity experiments were performed using the final assay conditions and the assay was robust and reproducible as judged by a Z' of 0.72.

Supplemental Figure S16 – PARP15 Assay Development

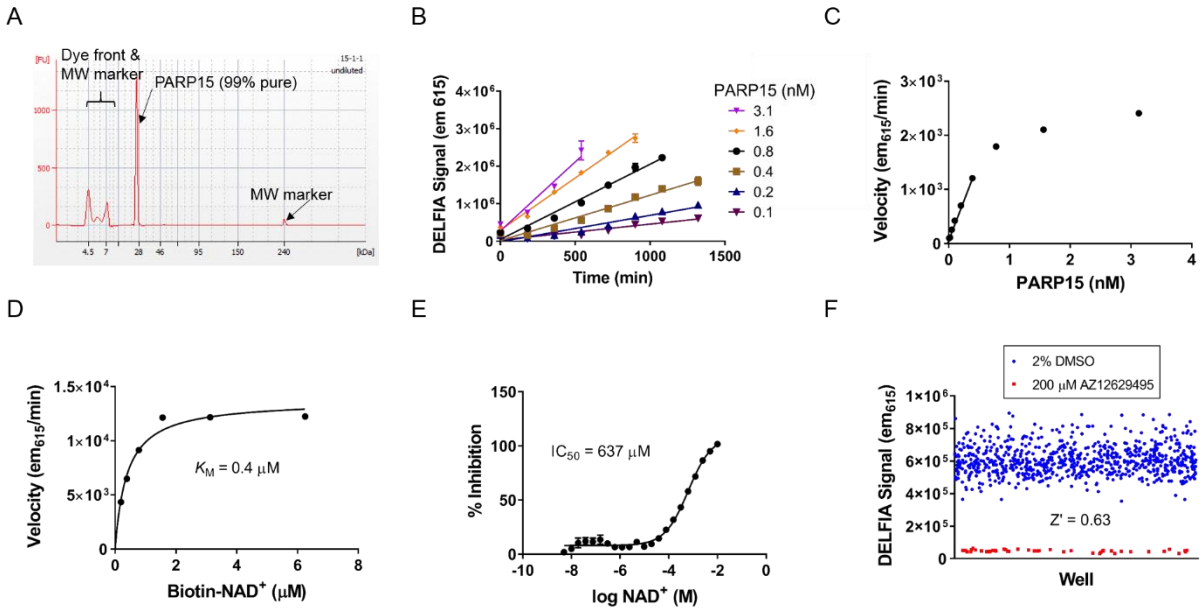

Figure S16. A) Recombinant PARP15 purified from *Sf9* cells via a His6 tag was 99% pure as judged by capillary electrophoresis. B) Linearity of product formation vs. time was evaluated at multiple enzyme concentrations. C) Velocity vs. enzyme concentration was plotted and the linear range of this relationship goes up to 0.4 nM enzyme. D) The K_M^{app} for biotin-NAD$^+$ was measured to be 0.4 µM. E) Unlabeled NAD$^+$ outcompetes incorporation of biotinylated NAD$^+$ under final assay conditions with an IC_{50} of 637 µM. F) Uniformity experiments were performed using the final assay conditions and the assay was robust and reproducible as judged by a Z' of 0.63.

Supplemental Figure S17 – Converting fluorescence units to molarity for PARP14 biotin-NAD$^+$ K_M

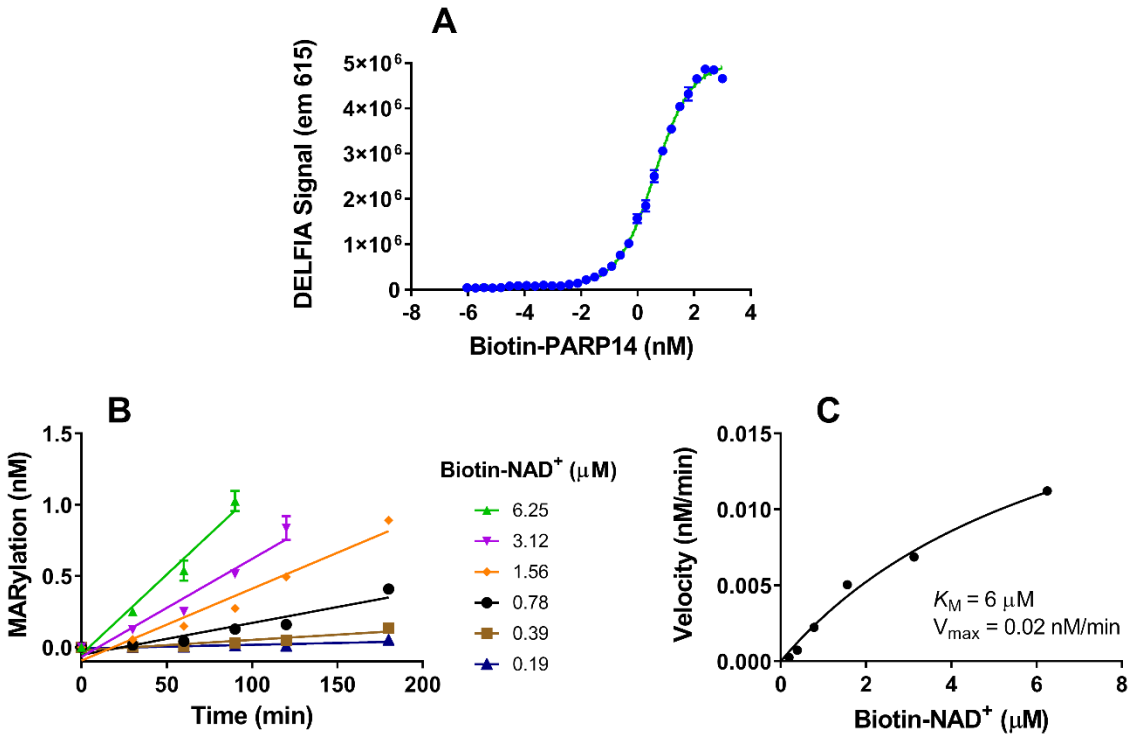

Figure S17. A) Recombinant His6-tagged PARP14 having the same amino sequence as the one used in the enzyme assay plus having an additional BirA tag where a single biotin was incorporated was used to create a standard curve. The standard curve was treated to the same DELFIA washing and detection protocol as the timecourse for the biotin-NAD$^+$ titration timecourse shown in panel B. B) A titration of biotin-NAD$^+$ was performed and the timecourse of MARylation, displayed in nM, of His6-tagged PARP14 lacking the BirA tag (same construct used in assay development if Figure S15) was generating by interpolating the standard curve shown in panel A. C) The K_M and V_{max} are calculated as a function of molarity. The K_M value of 6 μM measured here is within 3-fold of the K_M measured in another independent experiment expressed in fluorescence units shown in Figure S15.

Supplemental Figure S18 - Structures of key PARP inhibitors used during assay development

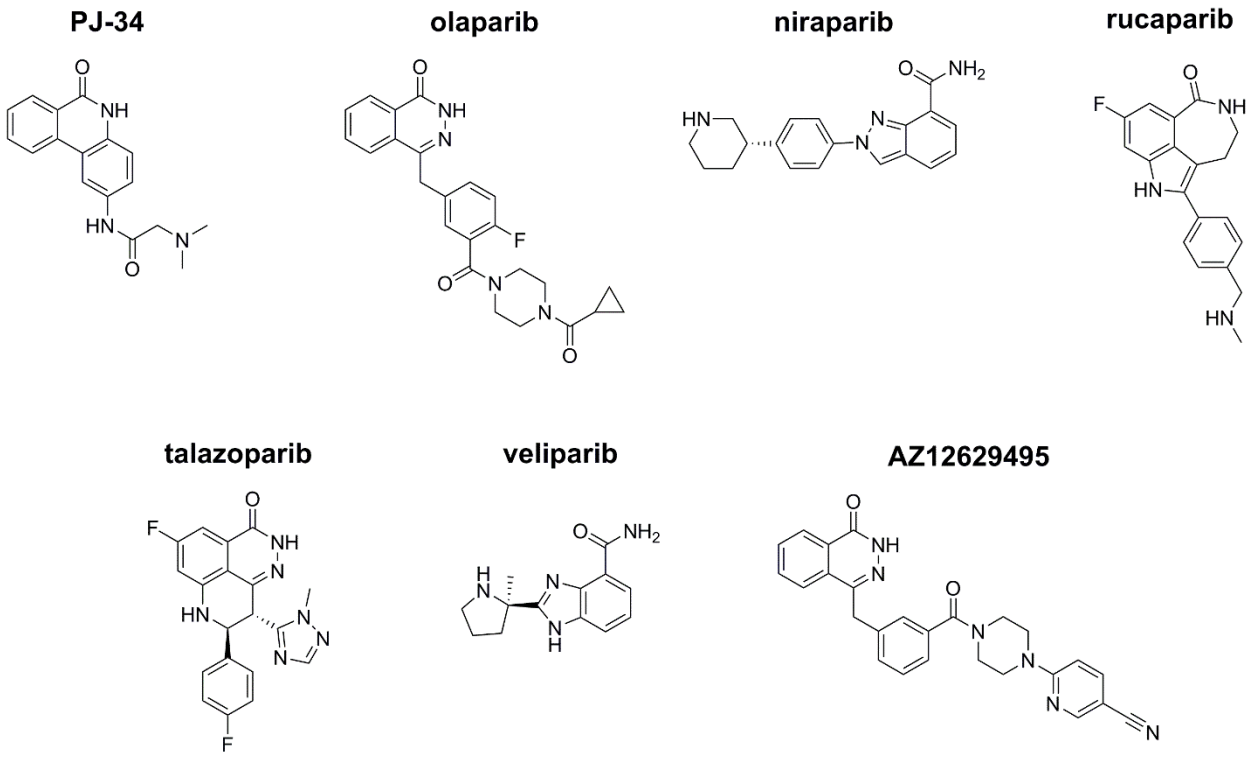

Figure S18. PJ-34 is a reported to be of modest potency[1], while olaparib, niraparib, rucaparib and talazoparib have been approved for use in human cancer treatment. Veliparib is in advanced clinical trials. AZ12629495 is a potent literature PARP inhibitor[2].

Supplemental Figure S19 - Correlation of SPR and enzyme assays

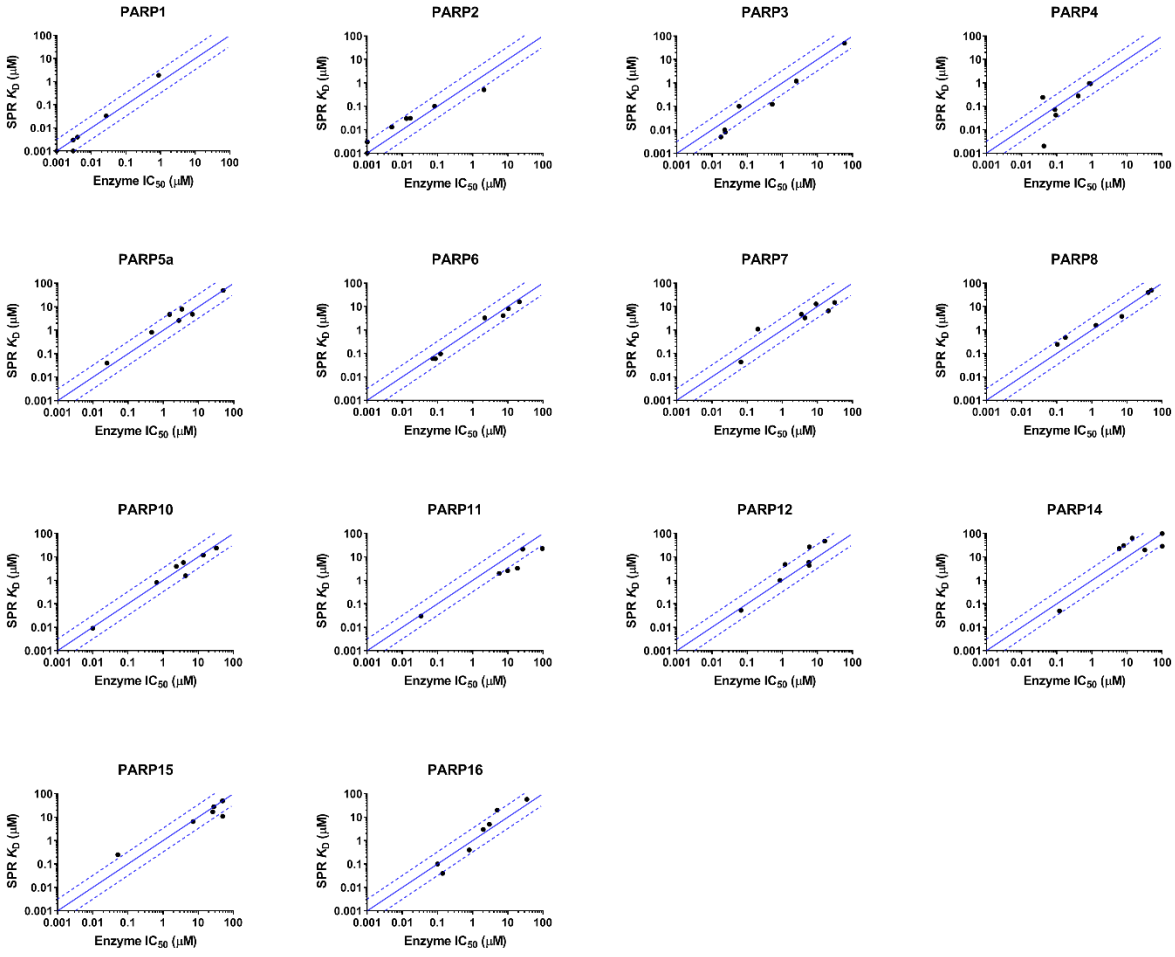

Figure S19. Full-length or catalytic domains for each PARP were captured on SPR chips either using biotin-Avi or His6 tags and binding affinity of a set of literature PARP1 inhibitors or a pan-monoPARP inhibitor was measured. The binding affinity for each compound was compared against the IC_{50} generated in the enzyme assays run at K_M^{app} or as close to possible to the K_M^{app} for biotin-NAD^+. Lines on the correlation plots are 1:1 (solid blue line) and 1:3 or 3:1 (dashed blue lines).

Supplemental Figure S20 - PARP9/DTX3L MARylation of ubiquitin is dependent on presence of all components needed to charge an E2 enzyme with ubiquitin.

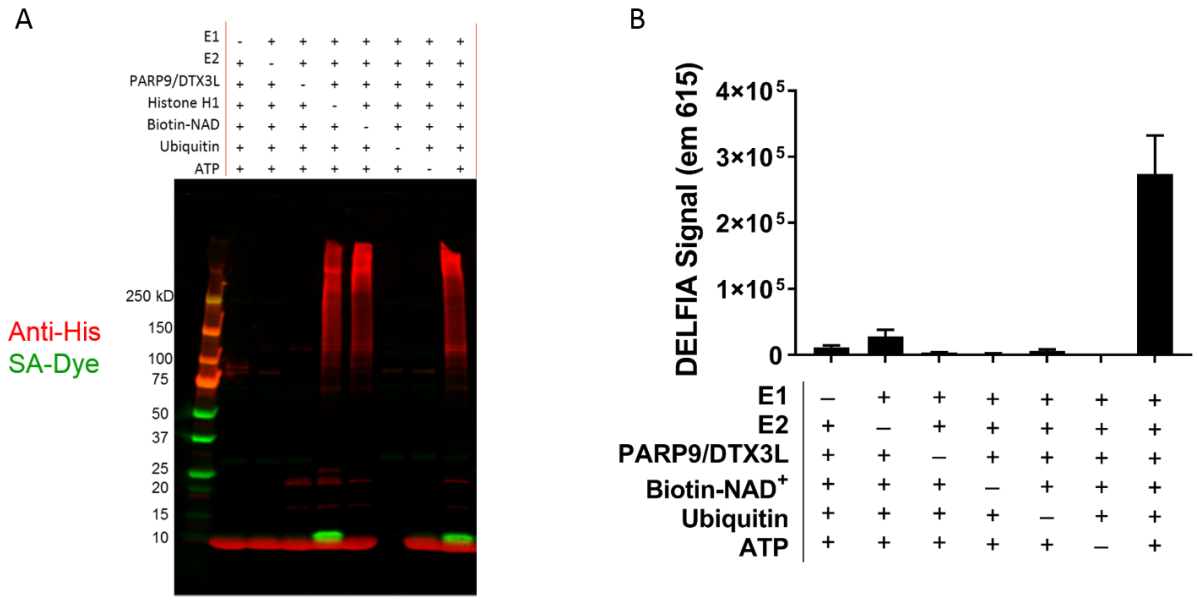

Figure S20. A series of samples containing all but one component needed to charge the E2 enzyme (UBE2D1) with His6-tagged ubiquitin were prepared and read out by A) far-Western blot or B) DELFIA.

Supplemental Figure S21 - Development of an assay to follow the ADP-ribosylation of ubiquitin by PARP9/DTX3L

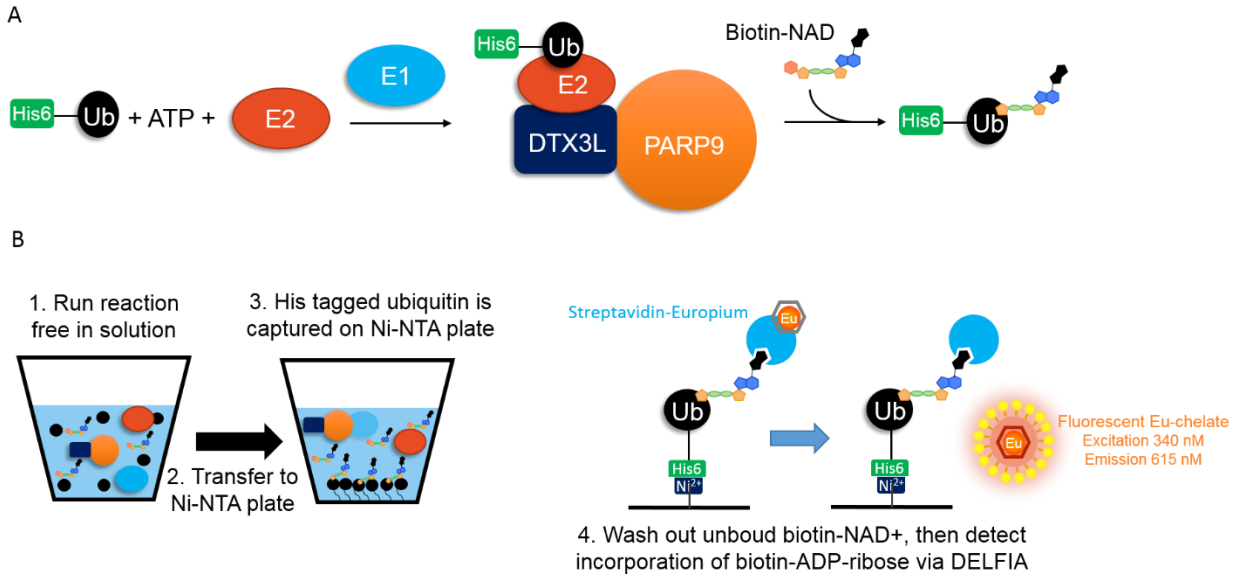

Figure S21. A) Biochemical schematic of the PARP9/DTX3L assay. The E1 activating enzyme hydrolyzes ATP to attach His6-tagged ubiquitin to the E2 conjugating enzyme. DTX3L, the E3 ligase in complex with PARP9, then directs the His6-ubiquitin-loaded E2 conjugating enzyme towards PARP9, which mono-ADP-ribosylates the C-terminus of the His6-ubiquitin. B) Workflow of PARP9 screening reaction. PARP9 reaction is run free in solution, then transferred to a Ni-NTA coated microplate which captures the His6-ubiquitin. The mono-ADP-ribosylated ubiquitin is detected using the same DELFIA readout used in the self-modification assays.

Supplemental Figure S22 - Schematic of nickel binding counterscreen assay

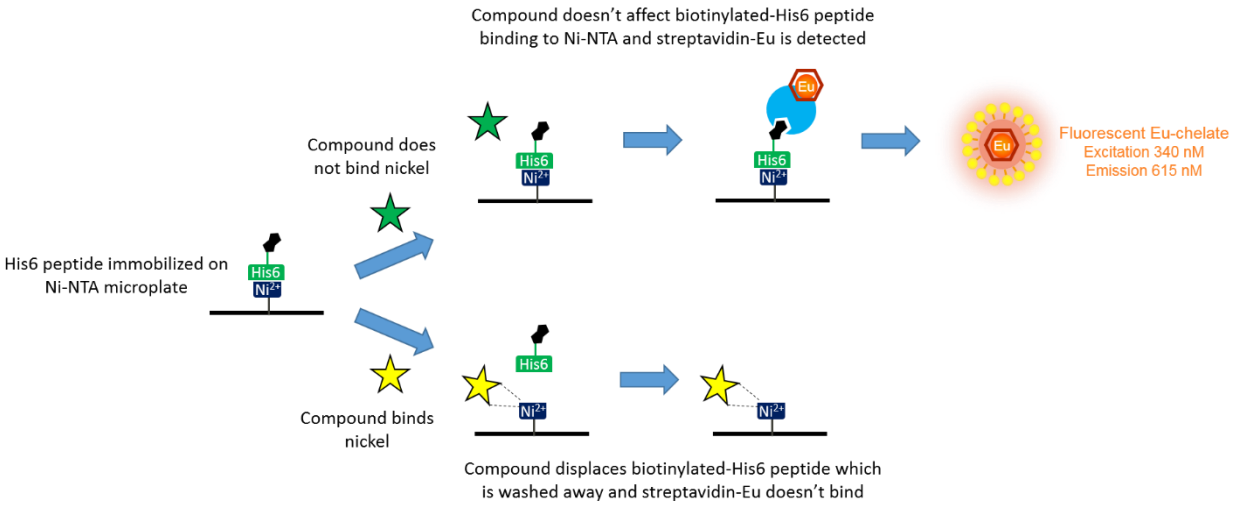

Figure S22. Counterscreen assay for compounds that bind Ni^{2+}. Since the capture of His6-tagged proteins underly the strategy for all the self-modification PARP assays and the PARP9/DTX3L assay, compounds that are capable of binding Ni^{2+} would prevent the binding of the proteins, and appear as hits during screening. To quickly identify these nuisance compounds, we developed a counterscreen assay following the displacement of biotinylated His6 peptide via the nickel-binding compounds. Test compounds are incubated with the peptide, and the remaining peptide bound to the microplate is detected using the same DELFIA readout used in the PARP assays.

Supplemental Table S1 – Protein constructs used in the enzyme and SPR assays*

PARP Name	Genbank accession number	Amino acid residues	Fusion tags	Expression System and Purification columns
PARP1	NM_001618.3	1-1014	N terminal-Flag-TEV-His6 MDYKDDDDKENLYFQSHHHHHH	*Sf9* Nickel, Flag
PARP2	NM_001042618.1	1-583	N terminal-Flag-TEV-His6 MDYKDDDDKENLYFQSHHHHHH	*Sf9* Nickel, Flag
PARP3	NM_005485	1-533	N-terminal His 6-PRX MAHHHHHHMDEKTTGWRGGHVVEGLAGEL EQLRARLEHHPQGQREPLEVLFQGP	*E. coli* Nickel, SEC
PARP4	NM_006437	226-566	N-terminal His6-TEV-G MHHHHHHSSGVDLGTENLYFQSG	*Sf21* Nickel, SEC
PARP5a	NM_003747.2	1001-1327	C-terminal His6 HHHHHH	*Sf9* Nickel, SEC, monoQ
PARP6	NM_020214	321-630	N-terminal MG-His6 MGHHHHHH	*E. coli* Nickel, SP, SEC
PARP7	NM_015508	456 – 657	N-His6-TEV-Avi MHHHHHHSSGVDLGTENLYFQSNAGLNDIFE AQKIEWHE	*E. coli* Wash inclusion bodies, Nickel, refold, Nickel
PARP8	NM_001178055.1	630-854	N-terminal MG-His6 MGHHHHHH	*E. coli* Nickel, SP, SEC
PARP10	NM_032789	808 – 1025	N-terminal His 6-TEV MHHHHHHSSGVDLGTENLYFQS	*E. coli* Nickel, monoQ, SEC
PARP11	NM_020367.5	1-338	N-terminal His6, C-terminal maltose binding protein MHHHHHH, MBP fusion	*Sf21* Nickel, SEC
PARP12	NM_022750	489 – 684	N terminal-His6-TEV-SM MAHHHHHHENLYFQSM	*Sf9* Nickel, SEC
PARP14	NM_017554	1611 – 1801	N terminal-His6-TEV (enzyme assay) MHHHHHHSSGVDLGTENLYFQS and N terminal-His6-TEV-Avi (SPR assay) MHHHHHHSSGVDLGTENLYFQSNAGLNDIF EAQKIEWHE	*E. coli* Nickel, SEC *E. coli* Nickel, TEV digestion, Biotinylation, Nickel, SEC
PARP15	NM_152615	481 – 678	N terminal His6-SSGVDLGT-TEV-SM MAHHHHHHSSGVDLGTENLYFQSM	*Sf9* Nickel, SEC
PARP16	NM_017851	5 – 279	N terminal-His6-TEV-SM (enzyme assay) MHHHHHHSSGVDLGTENLYFQSM and N terminal-His6-TEV-Avi (SPR assay) MHHHHHHSSGVDLGTENLYFQGLNDIFEAQKI EWHE	*E. coli* Nickel, SEC *E. coli* Nickel, TEV digestion, Biotinylation, Nickel, SEC

*unless specified in the fusion tags column, the same construct was used for both the enzyme and SPR assays.

Supplemental Table S2 – DNA oligomers used in selected enzyme assays

Assay	5' sequence	3' sequence
PARP1	ACCCTGCTGTGGGC/ideoxyU/GGAGAACAAGGTGAT	ATCACCTTGTTCTCCAHGCCCACA GCAGGGT
PARP2	/phosphate/GCCTATAGGC	/phosphate/GCCTATACCG
PARP3	/phosphate/GCTGGCTTCGTAAGAAGCCAGCTCGCGGTC AGCTTGCTGACCGCG	N/A

Supplemental Table S3 – Biotin-NAD$^+$ K_M^{app} and NAD$^+$ IC_{50} for each PARP assay

PARP Assay	Biotin-NAD$^+$ K_M^{app} (μM)	NAD$^+$ IC_{50} (μM)
PARP1	31	3.0
PARP2	5	50
PARP3	8	7.5
PARP4	14	21
PARP5a	5	400
PARP6	5	87
PARP7	2	1.1
PARP8	50	380
PARP9	22	1400
PARP10	3	460
PARP11	18	120
PARP12	12	73
PARP14	2	110
PARP15	1	640
PARP16	36	210

References

1. Garcia Soriano, F.; Virág, L.; Jagtap, P.; et al. Diabetic endothelial dysfunction: the role of poly(ADP-ribose) polymerase activation. *Nature Medicine* **2001,** *7*, 108-113.
2. Mikule, K., Wang, Z. Treatment of Cancer. **2016,** WO 2016/116602.